



# Study on a digital drilling test–based rock uniaxial compressive strength measurement method

Jun Yang<sup>1,2</sup> · Qian Qin<sup>1,3</sup> · Bei Jiang<sup>1,2,3,4</sup> · Yajun Wang<sup>1</sup> · Shucai Li<sup>3</sup>

Received: 28 December 2018 / Accepted: 28 January 2020 / Published online: 4 February 2020  
© Saudi Society for Geosciences 2020

## Abstract

Real-time and accurate measurement of the uniaxial compressive strength of rock on-site is the foundation of the design optimization and digital construction of the support structure in an underground project. Currently, effective methods to obtain the rock uniaxial compressive strength  $R_c$  in real-time on-site are scarce. Digital drilling test technology provides a new opportunity to solve this problem; however, the lack of a universal relational model for the drilling parameters versus  $R_c$  constrains further development of this technology. In this study, based on developed PDC bit for probing, the  $S_c$  parameters of rock cutting strength are proposed, and the relational equation between  $S_c$  and drilling parameters is deduced. Using an in-house-developed rock drilling test system, laboratory digital drilling tests for sandstone and mortar specimens with various strengths are performed. Based on the test results, a relational equation between  $R_c$  and  $S_c$  is developed. Subsequently, a relational model for drilling parameters versus  $R_c$  (the DP- $R_c$  model) is developed, and its effectiveness is verified. The results show that the average difference in the uniaxial compressive strength predicted by the DP- $R_c$  model versus the  $R_c$  measured in the uniaxial test is less than 10%, which proves the effectiveness of this model. On this basis, we propose a digital drilling test–based rock uniaxial compressive strength real-time measurement method that provides the foundation for the real-time and accurate measurement of the uniaxial compressive strength of the surrounding rock in underground projects.

**Keywords** Digital drilling · Uniaxial compressive strength · Drilling parameter · Rock cutting strength · Relational model

## Abbreviations

$V$	Drilling rate
$N$	Rotating speed
$M$	Drilling torque
$F$	Drilling pressure
$R_c$	Uniaxial compressive strength

$S_c$	Rock cutting strength
DP	Drilling parameters
$H$	Rock cutting depth $H$
$L$	Rock cutting range
$F_c$	Cutting force from the cutting blade on the front rock
$F_f$	The force from the cutting blade on the rock underneath
$\gamma$	The angle between the direction of the cutting force $F_c$ and the direction normal to the cutting blade surface
$\kappa$	The angle of inclination of the cutting blade
$\delta$	The angle between $F_f$ and the vertical
$M_c$	The cut torque
$M_f$	The friction torque
$F_c'$	Counterforce of $F_c$
$F_f'$	Counterforce of $F_f$
$R$	The drill bit radius
$L_i$	The length of the $i$ th row of the cutting edge
$r$	The distance from a section of a row of the cutting edge to the drill bit center O
$m$	The number of columns of drill bit cutting blades
Dh	The drilling depth
$M_f$	The initial torque

Responsible Editor: Longjun Dong

✉ Bei Jiang  
jiangbei519@163.com

- <sup>1</sup> State Key Laboratory for GeoMechanics and Deep Underground Engineering, China University of Mining & Technology-Beijing, Beijing 100083, China
- <sup>2</sup> State Key Laboratory for GeoMechanics and Deep Underground Engineering, China University of Mining & Technology, Xuzhou 221116, China
- <sup>3</sup> Research Center of Geotechnical and Structural Engineering, Shandong University, Jinan 250061, China
- <sup>4</sup> School of Civil Engineering and Architecture, University of Jinan, Jinan 250022, China

$M_S$	The average torque in the stable stage
$R_{Sc}$	The rock uniaxial compressive strength forecast value
$R^2$	Fitting degree
$\lambda$	The difference

## Introduction

Accurate and timely acquisition of underground engineering data and deal with effective analysis methods are great significance for maintaining the safety and stability of underground engineering (Dong et al. 2018, 2019). Uniaxial compressive strength is a basic parameter that describes the surrounding rock strength during drilling operations. Real-time and accurate measurement of this parameter on-site is necessary to support parameter design, construction method selection, and digital construction. Laboratory testing is a basic uniaxial compressive strength testing method (Pincus 1993; Wijk 1980). However, laboratory testing requires core sampling on-site and subsequent transmission of the samples to the laboratory for testing and analysis. Therefore, laboratory testing presents several disadvantages, such as a long turn-around cycle, a high cost, and the inability to perform real-time testing in the disturbed rock after excavation. A fast and accurate method for surrounding rock uniaxial compressive strength on-site measurement has significant engineering importance. A point load test is one of the primary rock strength on-site measurement methods (Al-Derbi and de Freitas 1999; Basu and Aydin 2006; Bieniawski 1974; Diamantis et al. 2009; Kahraman 2014; Karaca et al. 2008; Panek and Fannon 1992; Singh and Singh 1993). However, under a point load, the specimen develops tensile stress-induced splitting failure (Guo 2003), which presents a failure mechanism significantly different from rock compression failure. This leads to a significant difference in conversion coefficients for point load strength and uniaxial compressive strength for various types of rocks (Singh et al. 2012; Broch and Franklin 1972; Quane and Russell 2003), which limits the application conditions for the method. Additionally, the point load test measures the strength of rock under the surrounding rock surface; however, for deep surrounding rock, a core sample is required, which affects the actual rock stress state. Therefore, further study on the fast and accurate measurement of the surrounding rock uniaxial compressive strength on-site is in high demand.

Drilling parameters are the operational parameters of a drilling rig during drilling operations, e.g., the drilling rate, the rotating speed, the torque, and the propulsive force. In digital drilling, the drilling parameters are monitored during drilling (Gui et al. 2002; Suzuki et al. 1995; Yang et al. 2012; Yue et al. 2004; Kovalyshen 2013), and some parameters are controlled quantitatively. Numerous on-site and

laboratory digital drilling tests have shown that drilling parameters and rock mechanical parameters are closely related (Teale 1965; Aalizad and Rashidinejad 2012; Kahraman 1999; Wyk et al. 2014). These findings provide a new method for a technique for real-time acquisition of the surrounding rock uniaxial compressive strength on-site, which involves obtaining the rock uniaxial compressive strength in real time using digital drilling test technology. To date, most researchers have conducted preliminary qualitative studies on the relation between certain drilling parameters and the rock uniaxial compressive strength (Chen and Yue 2015; Kahraman et al. 2003; Tan et al. 2005). However, systematic studies and quantitative descriptions of the relation between the two are scarce. Some researchers have attempted to create a relational model for the rock compressive strength and the drilling parameters from the perspectives of statistical analysis (Huang and Wang 1997; Monjezi et al. 2012; Mostofi et al. 2011; Yaşar et al. 2011) and energy analysis (Detournay and Defourny 1991; Karasawa et al. 2002; Tan et al. 2007). However, the existing relational models depend on the drilling rig type and the control variables of the drilling parameters; i.e., if the drilling rig or a control variable of the drilling parameters during drilling are changed, the model may not be applicable. This limits further development of digital drilling test technology.

The key to on-site real-time surrounding rock uniaxial compressive strength measurement based on digital drilling tests is to develop a universal quantitative relation between the drilling parameters and the rock uniaxial compressive strength parameter. To achieve that goal in this study, based on developed PDC bit for probing, the  $S_c$  parameters of rock cutting strength are proposed, and the relational equation between  $S_c$  and drilling parameters is deduced. Using an in-house-developed rock drilling test system, laboratory digital drilling tests for sandstone and mortar specimens with various strengths are performed. Based on the test results, relational equation for  $R_c$  and  $S_c$  are developed. Subsequently, a relational model for the drilling parameters and  $R_c$  (DP- $R_c$  model) is created and its validity and accuracy are verified by experiments. We propose a digital drilling test-based rock uniaxial compressive strength measurement method. This study provides the foundation for digital drilling test technology implementation as well as for the fast and accurate measurement of surrounding rock mechanical parameters at construction sites.

## The relation formula between $S_c$ and drilling parameters

A new-type PDC bit is designed for probing, as shown in Fig. 1. The cutting edge uses square polycrystalline diamond

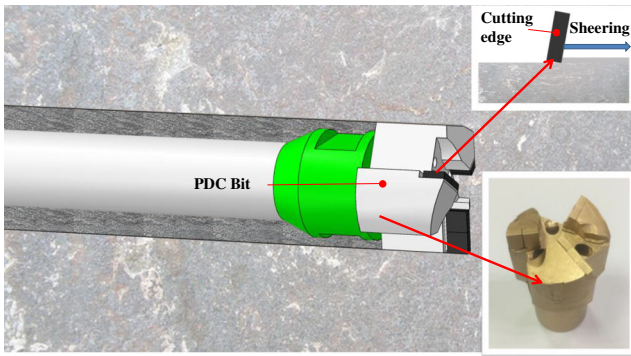


Fig. 1 Polycrystalline diamond compact drill bits (PDC bits)

compact, whose shape and stress characteristics will not be changed even if it is abraded during the drilling process. Therefore, it can minimize the effects of diamond compact abrasion on test data. Meanwhile, using the square polycrystalline diamond compact is also convenient for carrying out mechanical analysis of rock cutting process. Usually, the width of each row of the cutting edge in the drill bit is more than 10 times the instantaneous cutting depth of the cutting edge of drilling bit (hereinafter referred to as the rock cutting depth  $H$ ). As shown in Fig. 1,  $H$  and the rock cutting range  $L$  are far smaller than the width of each row of the cutting edge. Therefore, in each cycle of rock cutting, the cutting edge follows an approximately linear path. Because  $H$  is usually small, the rock in front of the cutting edge demonstrates mostly ductile failure. The rock cutting problem basically satisfies the conditions of a plane strain problem. The process of cutting rock by the cutting edge of PDC bit at any moment is shown in Fig. 2.

In Fig. 2,  $F_c$  is the cutting force from the cutting blade on the front rock;  $F_f$  is the force from the cutting blade on the rock underneath;  $\gamma$  is the angle between the direction of the cutting force  $F_c$  and the direction normal to the cutting blade surface;  $\kappa$  is the angle of inclination of the cutting blade; and  $\delta$  is the angle between  $F_f$  and the vertical, which is also the friction angle between the cutting blade and the rock.

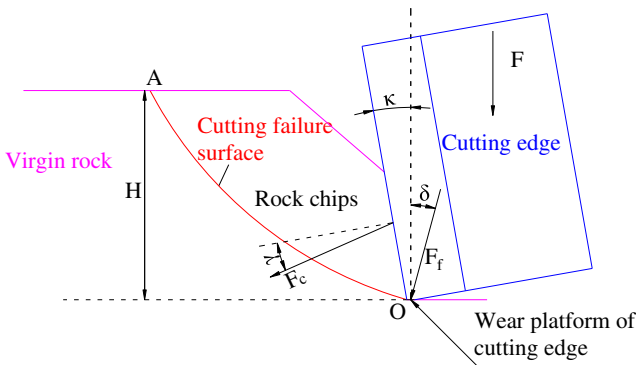


Fig. 2 Rock cutting mechanical model

### Solution for the drill bit torque $M$

The torque  $M$  required for rock cutting consists of two components, the cut torque  $M_c$  and the friction torque  $M_f$ , as shown in Fig. 2. The cut torque  $M_c$  is the drilling rig moment for rock cutting, which is obtained by calculating the moment of the horizontal component of  $F'_c$  ( $F'_c$  is counterforce of  $F_c$ ) with respect to the drill bit center;  $M_f$  is the moment exerted by the drilling rig to overcome the friction between the drill bit and the rock below, which is obtained by calculating the moment of the horizontal component of  $F'_f$  ( $F'_f$  is counterforce of  $F_f$ ) with respect to the drill bit center.

As shown in Fig. 3, the drill bit radius is  $R$ ; there are 3 rows of cutting edges; the length of the  $i$ th row of the cutting edge is  $L_i$ ; and the distance from a section of a row of the cutting edge to the drill bit center  $O$  is  $r$ . In any segment  $dr$ , the torque on the drill bit is as follows:

$$dM = dM_c + dM_f = F'_c r \cos(\kappa + \gamma) dr + F'_f r \sin \delta dr \quad (1)$$

The integral of the moment  $dM$  along the cutting edge length is calculated and the moments at all row cutting edges are summed to obtain the overall drilling rig torque  $M$  as follows:

$$M = \sum_{i=1}^3 \int_{R-L_i}^R (F'_c \cos(\kappa + \gamma) + F'_f \sin \delta) r dr = \frac{1}{2} [F'_c \cos(\kappa + \gamma) + F'_f \sin \delta] [2R(L_1 + L_2 + L_3) - (L_1^2 + L_2^2 + L_3^2)] \quad (2)$$

### Solution for the drilling pressure $F$

The drilling pressure  $F$  is the pressure exerted by the drilling rig to overcome the vertical component of  $F'_c$  and  $F'_f$ . For the drill bit shown in Fig. 2,  $F$  is as follows:

$$F = [F'_c \sin(\kappa + \gamma) + F'_f \cos \delta] (L_1 + L_2 + L_3) \quad (3)$$

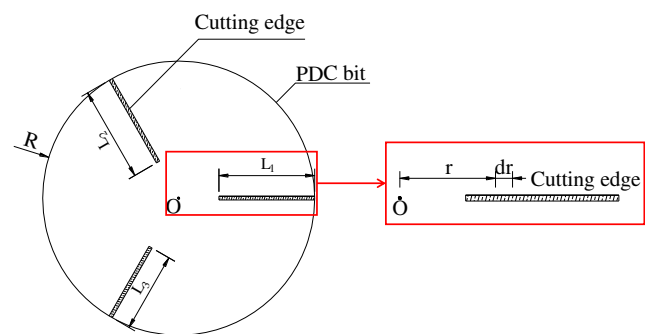


Fig. 3 Schematic diagram of the drill bit and one row of the cutting edge

### Solution for the cutting strength $S_c$

Equations (2) and (3) are combined to eliminate the unknown force  $F'_f$ :

$$M = \frac{1}{2} F'_c [\cos(\kappa + \gamma) - \sin(\kappa + \gamma) \tan \delta] [2R(L_1 + L_2 + L_3) - (L_1^2 + L_2^2 + L_3^2)] + \frac{1}{2} F \tan \delta \left( 2R - \frac{L_1^2 + L_2^2 + L_3^2}{L_1 + L_2 + L_3} \right) \quad (4)$$

The ultimate cutting force  $F_c$  from the cutting blade on the front rock is then as follows:

$$F_c = F'_c = \frac{2M - F \tan \delta \left( 2R - \frac{L_1^2 + L_2^2 + L_3^2}{L_1 + L_2 + L_3} \right)}{[\cos(\kappa + \gamma) - \sin(\kappa + \gamma) \tan \delta] [2R(L_1 + L_2 + L_3) - (L_1^2 + L_2^2 + L_3^2)]} \quad (5)$$

The rock cutting strength  $S_c$  physically represents the ultimate cutting force needed to cut a unit depth of rock:

$$S_c = \frac{F_c}{H} \quad (6)$$

$$H = \frac{V}{mN} \quad (7)$$

where  $V$  is the drilling rate;  $N$  is the rotating speed; and  $m$  is the number of columns of drill bit cutting blades. In this study, a drill bit with  $m = 3$  was used.

Based on Eqs. (5), (6), and (7),  $S_c$  is as follows:

$$S_c = \frac{3N \left[ 2M - F \tan \delta \left( 2R - \frac{L_1^2 + L_2^2 + L_3^2}{L_1 + L_2 + L_3} \right) \right]}{V [\cos(\kappa + \gamma) - \sin(\kappa + \gamma) \tan \delta] [2R(L_1 + L_2 + L_3) - (L_1^2 + L_2^2 + L_3^2)]} \quad (8)$$

### Digital drilling test

To study the relation between the rock uniaxial compressive strength  $R_c$  and the rock cutting strength  $S_c$  systematically, a digital drilling test-based rock uniaxial compressive strength real-time measurement method is developed. Using an in-house-developed rock drilling test system, digital drilling tests for sandstone and mortar specimens with various strengths are performed.

### Test equipment

The equipment used in the test is the in-house-developed rock drilling test system shown in Fig. 4. This system includes a drilling system, a loading system, a pressure chamber device, and a monitoring control system. It can test the correlation between drilling parameters and rock mechanical parameters under various control modes. This drilling rig is controlled by

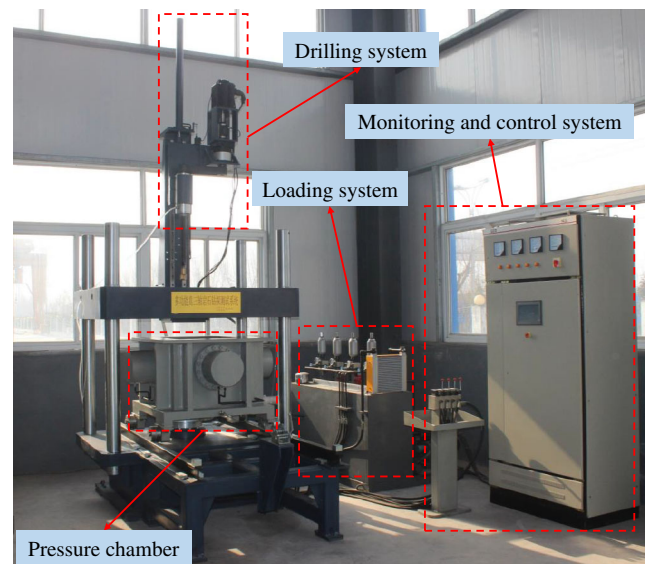


Fig. 4 Rock drilling test system

a hydraulic pressure servo system. It can provide a maximum rotational speed of 400 r/min, a maximum drilling thrust of 50 kN, and a maximum torque of 400 N·m. It can test any specimen whose length × width × height is less than or equal to 300 mm × 300 mm × 600 mm.

The drill bit used in this test is the new polycrystalline diamond compact (PDC) drill bit designed by authors, as shown in Fig. 1. Parameters of the drill bit are shown in Table 1.

### Design of the test plan

Sandstone and mortar specimens, 36 groups in total, are tested. Among them, there are 8 groups of sandstone specimens, S1~S8. The mortar specimens have 7 different strength grades, listed in Table 2. Each grade type has 4 groups; there are 28 groups in total, J1~J28. The sample dimensions are 150 mm × 150 mm × 230 mm (length × width × height).

Note that the cement strength grade for cement mortar whose strength grade is M15 or below is 32.5, and the cement strength grade for cement mortar whose strength grade exceeds M15 is 42.5.

For each specimen, the rock drilling test system is employed to perform the digital drilling test to a drilling depth of 110 mm. The coring drill bit is then used to collect a core sample from the remaining part of the specimen, and a

Table 1 PDC bit parameters

Bit parameters	$R$	$L_1$	$L_2$	$L_3$	$\kappa$
Sizes	30 mm	18 mm	18 mm	27 mm	15°

**Table 2** Different mortar strength ratio

Mortar strength grade	Cement (kg/m <sup>3</sup> )	Sand (kg/m <sup>3</sup> )	Water (kg/m <sup>3</sup> )
M5	215	1450	300
M7.5	245		
M10	275		
M15	310		
M20	370		
M25	385		
M30	455		

standard rock core specimen is prepared. A uniaxial compression test is performed to obtain the uniaxial compressive strength  $R_c$  of the specimen. Example test specimens after drilling are shown in Fig. 5.

There are 36 groups of sandstone and mortar specimens. Six groups of sandstone specimens and 22 groups of mortar specimens are randomly selected for the drilling tests used to develop the relational equations and obtain the DP- $R_c$  model. The remaining 2 groups of sandstone specimens and 6 groups of mortar specimens are used to verify the effectiveness of the DP- $R_c$  model.

## Test results

### Test result selection

The tests are based on the mode that controls the drilling rate  $V$ , the drill rotating speed  $N$ , the collection torque  $M$ , and the thrust  $F$ . The typical test data for plan  $S_3$  are used as an example to obtain the drilling parameter curves shown in Fig. 6, where  $D_h$  is the drilling depth. The data in Fig. 6 a show that when the drill bit first contacts the specimen,  $V$  is small. After the drill reaches a certain depth,  $V$  reaches a steady-state condition at the predefined rate of 85 mm/min, thus satisfying the test requirement.

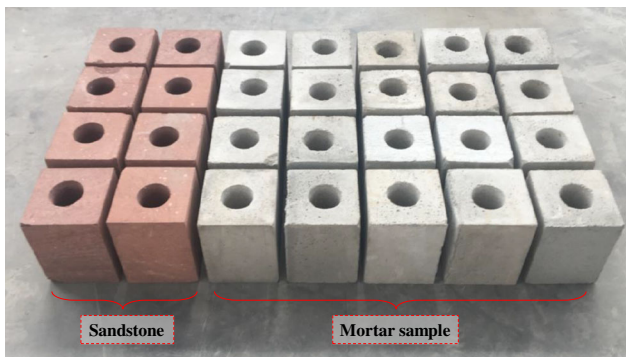


**Fig. 5** Test specimens after drilling

The data in Fig. 6 b show that  $N$  is constant at 150 r/min, also satisfying the test requirement.

Figure 6 c shows the measured variation curve of  $M$  versus  $D_h$  when drilling into this specimen. Figure 6 d shows the variation curve of  $F$  versus  $D_h$ . The variation rules for  $M$  and  $F$  with respect to  $D_h$  are similar, showing two phases.

① Before the drill bit enters the rock,  $M$  and  $F$  are small; after it drills into the rock,  $M$  and  $F$  increase sharply in a small  $D_h$ . This is the rising stage.

② After the drill bit reaches a shallow drilling depth,  $M$  and  $F$  reach a stable stage. During this stable stage, when  $D_h$  increases,  $M$  fluctuates slightly around a stable value.

The  $M$  and  $F$  of rock specimens were monitored by test. The test calculation methods for  $M$  and  $F$  are identical. The calculation for  $M$  is used as an example to illustrate the process. Before the rock specimen is drilled, the initial torque is  $M_I$ , the average torque in the stable stage is  $M_S$ , and the specimen torque test value is  $M = M_S - M_I$ . Using the data for the specimen in Fig. 8 as an example,  $M_I = 24.81 \text{ N}\cdot\text{m}$ ,  $M_S = 65.5 \text{ N}\cdot\text{m}$ , and  $M = M_S - M_I = 40.69 \text{ N}\cdot\text{m}$ .

### $S_c$ equation's parameter selection

The test specimens used in this paper are sandstone and cement mortar specimens, which have the similar lithology as the specimens used by Huang et al. (2013) and Yahiaoui et al. (2016). Therefore, based on their research results, authors select  $\gamma = 12^\circ$  and  $\delta = 12^\circ$  preliminarily. The bit parameters in the  $S_c$  equation are selected according to Table 1.

### Digital drilling test and result analysis

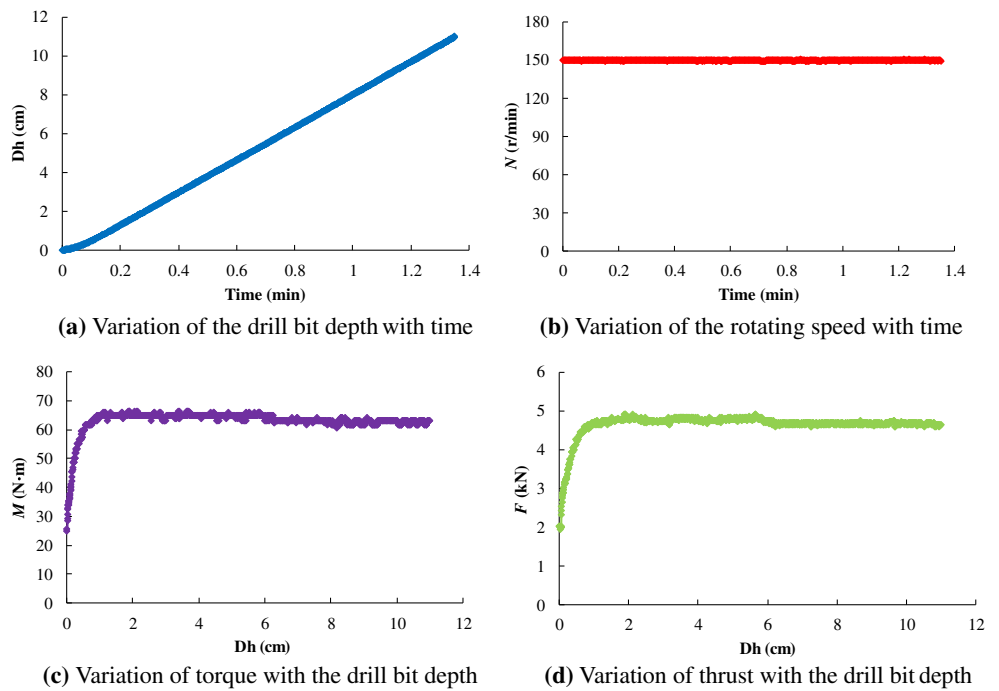
Based on the test plan, a system test is performed to obtain drilling parameters  $V$ ,  $N$ ,  $M$ , and  $F$  for each specimen. The drilling parameters are substituted into Eq. (8) to obtain  $S_c$ . The detailed results are listed in Table 3.

### Analysis of the relation between $R_c$ and $S_c$

The results from the digital drilling test and the rock uniaxial compressive strength  $R_c$  from the uniaxial test are compared with the calculated rock cutting strength  $S_c$  to create the quantitative relational equations for  $S_c$  and  $R_c$ .

Using the  $R_c$  and  $S_c$  test data for each group of specimens in Table 3, a scatter diagram ( $S_c$  on the  $x$ -axis and  $R_c$  on the  $y$ -axis), used to determine the relation between  $S_c$  and  $R_c$ , is shown in Fig. 7. The data show that  $R_c$  and  $S_c$  have a positive linear relation; i.e.,  $R_c$  increases as  $S_c$  increases. The variation rate of  $R_c$  versus  $S_c$  is 0.4007 with a fitting degree of  $R^2 =$

**Fig. 6** The drilling parameter curves. **a** Variation of the drill bit depth with time. **b** Variation of the rotating speed with time. **c** Variation of torque with the drill bit depth. **d** Variation of thrust with the drill bit depth



0.9687. Therefore, the test data have a low level of discreteness and a high degree of fit.

Based on the optimal fitting curve for  $S_c$  and  $R_c$ , the relational equation for  $S_c$  and the rock uniaxial compressive

strength forecast value  $R_{Sc}$  is as follows:

$$R_{Sc} = 0.4007S_c - 3.9884 \tag{9}$$

**Table 3** Results from the digital drilling tests and mechanical analytical model for rock cutting

Sample type	Number	$V$ (mm/min)	$N$ (r/min)	$M$ (N·m)	$F$ (kN)	$S_c$ (MPa)	$R_c$ (MPa)
M5	J <sub>1</sub>	148.46	50	18.92	0.02	19.94	1.9
	J <sub>2</sub>	177.89	100	14.43	0.01	25.42	2
	J <sub>3</sub>	185.07	100	12.98	0.01	21.97	1.94
	J <sub>4</sub>	174.69	100	13.99	0.01	25.09	1.99
M7.5	J <sub>5</sub>	124.80	50	17.01	0.03	21.26	2.37
	J <sub>6</sub>	87.94	100	7.30	0.02	25.78	2.58
	J <sub>7</sub>	105.70	100	6.19	0.03	18.04	3.29
M10	J <sub>9</sub>	81.52	50	17.05	0.03	32.64	6.7
	J <sub>10</sub>	103.09	100	12.22	0.02	37.01	7.2
	J <sub>11</sub>	112.75	100	10.13	0.03	27.88	6.24
M15	J <sub>12</sub>	130.77	100	14.67	0.03	34.97	6.99
	J <sub>13</sub>	83.85	50	28.77	2.79	32.72	10.23
	J <sub>14</sub>	83.95	100	16.42	2.66	21.10	10.05
	J <sub>15</sub>	132.05	100	22.34	2.15	32.44	10.54
M20	J <sub>16</sub>	118.08	100	21.44	2.07	34.73	10.6
	J <sub>17</sub>	83.91	50	45.43	2.23	68.13	23.54
	J <sub>18</sub>	83.65	100	29.89	2.33	76.88	30.81
M25	J <sub>19</sub>	111.42	100	35.88	3.01	66.79	22.43
	J <sub>21</sub>	83.46	50	43.66	3.44	55.93	21.66
	J <sub>22</sub>	84.23	100	26.15	1.20	79.45	27.8
M30	J <sub>23</sub>	137.82	100	38.30	3.16	58.08	22.22
	J <sub>25</sub>	84.64	50	41.49	0.85	70.65	27.71
	J <sub>26</sub>	82.88	100	25.99	0.51	90.73	35.21
Sandstone	J <sub>27</sub>	137.84	100	31.16	1.49	57.31	22.73
	S <sub>1</sub>	79.97	50	103.08	5.59	157.99	58.09
	S <sub>3</sub>	84.07	150	40.69	2.65	167.98	59.95
	S <sub>5</sub>	84.90	250	28.00	2.15	178.50	61.91
	S <sub>6</sub>	84.41	300	23.78	2.05	172.95	60.88
	S <sub>7</sub>	110.72	100	65.20	5.48	122.05	51.41
	S <sub>8</sub>	136.47	100	73.96	6.10	113.38	49.8

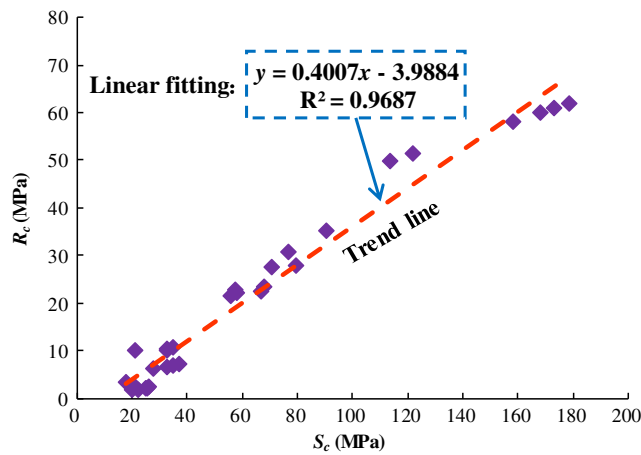


**Fig. 7** Analysis of the relation between the rock uniaxial compressive strength  $R_c$  and the rock cutting strength  $S_c$

Equation (8) is substituted into Eq. (9) to obtain the DP- $R_c$  model as follows:

$$R_{Sc} = \frac{1.2021N \left[ 2M - F \tan \delta \left( 2R - \frac{L_1^2 + L_2^2 + L_3^2}{L_1 + L_2 + L_3} \right) \right]}{V [\cos(\kappa + \gamma) - \sin(\kappa + \gamma) \tan \delta] [2R(L_1 + L_2 + L_3) - (L_1^2 + L_2^2 + L_3^2)]} - 3.9884 \quad (10)$$

### DP- $R_c$ model verification

DP- $R_c$  model verification is performed using the remaining 8 groups of specimens. The rock uniaxial compressive strength forecast value  $R_{Sc}$  is obtained via Eq. (10). To quantitatively evaluate the difference between the results of the DP- $R_c$  model and the conventional measurement method, the difference  $\lambda$  between  $R_{Sc}$  and  $R_c$  is defined as follows:

$$\lambda = \left| \frac{R_{Sc} - R_c}{R_c} \right| \times 100\% \quad (11)$$

The drilling parameters  $V$ ,  $N$ ,  $M$ , and  $F$  and  $R_c$ ,  $R_{Sc}$ , and  $\lambda$  are listed in Table 4.

The comparison of  $R_{Sc}$  with  $R_c$  is shown in Fig. 8. An analysis of the data in Fig. 8 shows that the difference between

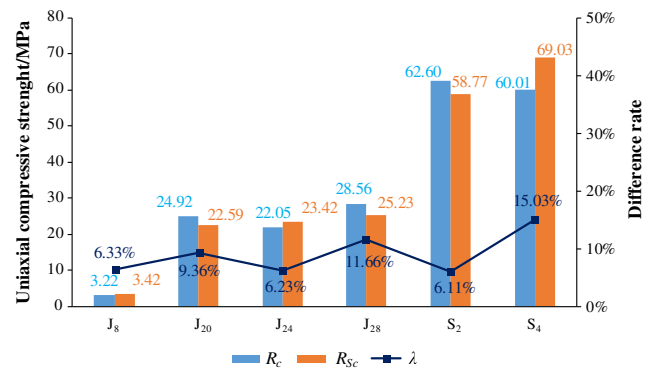


**Fig. 8** Comparison analysis of  $R_{Sc}$  and  $R_c$

$R_{Sc}$  and  $R_c$  is small. The average is  $\bar{\lambda} = 9.12\%$ , i.e., less than 10%. This validates the effectiveness of the DP- $R_c$  model.

Hence, based on the DP- $R_c$  model and the drilling parameters obtained via an on-site drilling test, real-time and effective measurement of the rock uniaxial compressive strength is feasible. This method provides the foundation for real-time and accurate measurement of surrounding rock uniaxial compressive strength on-site for underground projects.

### Conclusions

- (1) In this study, based on developed PDC bit for probing, the  $S_c$  parameters of rock cutting strength are proposed, and the relational equation between  $S_c$  and drilling parameters is deduced.
- (2) Using an in-house-developed rock drilling test system, laboratory digital drilling tests for sandstone and mortar specimens with various strengths are performed. The relation between the rock uniaxial compressive strength parameters  $R_c$  and  $S_c$  is investigated, resulting in a relational equation for  $R_c$  and  $S_c$  that is used to develop the DP- $R_c$  model.
- (3) The effectiveness of the DP- $R_c$  model is verified via digital drilling tests. The results show that the average difference between the uniaxial compressive strength  $R_{Sc}$  predicted by the DP- $R_c$  model and the  $R_c$  measured by the uniaxial test is less than 10%. This validates the effectiveness of the DP- $R_c$  model.

**Table 4** Data for verification of the relational model for the drilling parameters and  $R_{Sc}$

Sample type	Number	$V$ (mm/min)	$N$ (r/min)	$M$ (N·m)	$F$ (kN)	$R_c$ (MPa)	$R_{Sc}$ (MPa)	$\lambda$
M7.5	J <sub>8</sub>	138.95	100	8.38	0.05	3.22	3.42	6.33%
M20	J <sub>20</sub>	137.76	100	43.29	3.51	24.92	22.59	9.36%
M25	J <sub>24</sub>	112.42	100	34.25	2.41	22.05	23.42	6.23%
M30	J <sub>28</sub>	114.25	100	30.32	0.94	28.56	25.23	11.66%
Sandstone	S <sub>2</sub>	84.41	100	53.10	2.72	62.60	58.77	6.11%
	S <sub>4</sub>	84.09	200	32.28	1.95	60.01	69.03	15.03%

- (4) A digital drilling test-based rock uniaxial compressive strength measurement method is proposed. This method provides technical support for measurement of surrounding rock uniaxial compressive strength parameters on-site in underground projects.

**Funding information** This study was supported by the Natural Science Foundation of China (grant numbers 51674265, 51704125, 51674154, 51874188); the Natural Science Foundation of Shandong Province, China (grant numbers 2018GGX109001, ZR2017QEE013, 2017GGX30101); and the State Key Laboratory for GeoMechanics and Deep Underground Engineering, China University of Mining and Technology (grant number SKLGDUEK1717).

## References

- Aalizad SA, Rashidinejad F (2012) Prediction of penetration rate of rotary-percussive drilling using artificial neural networks—a case study. *Arch Min Sci* 57:715–728
- Al-Derbi MS, de Freitas MH (1999) Use of the boussinesq equation for determining the distribution of stress within a diametrical point load test. *Rock Mech Rock Eng* 32:257–265
- Basu A, Aydin A (2006) Predicting uniaxial compressive strength by point load test: significance of cone penetration. *Rock Mech Rock Eng* 39:483–490
- Bieniawski ZT (1974) Estimating the strength of rock materials. *J South Afr Inst Min Metall* 74:312–320
- Broch E, Franklin JA (1972) The point-load strength test. *Int J Rock Mech Min Sci Geomech Abstr* 9:669–697
- Chen J, Yue ZQ (2015) Ground characterization using breaking-action-based zoning analysis of rotary-percussive instrumented drilling. *Int J Rock Mech Min Sci* 75:33–43
- Detournay E, Defourny P (1991) A phenomenological model for the drilling action of drag bits. *Int J Rock Mech Min Sci Geomech Abstr* 29:13–23
- Diamantis K, Gartzos E, Migiros G (2009) Study on uniaxial compressive strength, point load strength index, dynamic and physical properties of serpentinites from Central Greece: test results and empirical relations. *Eng Geol* 108:199–207
- Dong LJ, Sun DY, Li XB, Ma J, Zhang LY, Tong XJ (2018) Interval non-probabilistic reliability of surrounding jointed rockmass considering microseismic loads in mining tunnels. *Tunn Undergr Space Technol* 81:326–335
- Dong LJ, Zou W, Li XB, Shu WW, Wang ZW (2019) Collaborative localization method using analytical and iterative solutions for microseismic/acoustic emission sources in the rockmass structure for underground mining. *Eng Fract Mech* 210:95–112
- Gui MW, Soga K, Bolton MD, Hamelin JP (2002) Instrumented borehole drilling for subsurface investigation. *J. Geotech Geoenviron Eng* 128:283–291
- Guo ML (2003) Discussion on adaptability of point load test of rocks. *Rock Soil Mech* 24:488–489 (in Chinese)
- Huang SL, Wang ZW (1997) The mechanics of diamond core drilling of rocks. *Int J Rock Mech Min Sci* 34:612
- Huang H, Lecampion B, Detournay E (2013) Discrete element modeling of tool-rock interaction I: rock cutting. *Int J Numer Anal Meth Geomech* 37:1913–1929
- Kahraman S (1999) Rotary and percussive drilling prediction using regression analysis. *Int J Rock Mech Min Sci* 36:981–989
- Kahraman S (2014) The determination of uniaxial compressive strength from point load strength for pyroclastic rocks. *Eng Geol* 170:33–42
- Kahraman S, Bilgin N, Feridunoglu C (2003) Dominant rock properties affecting the penetration rate of percussive drills. *Int J Rock Mech Min Sci* 40:711–723
- Karaca Z, Yilmaz NG, Goktan RM (2008) Comparison of averaging procedures for point load testing of rock. *Geotech Test J* 31:456–460
- Karasawa H, Ohno T, Kosugi M, Rowley JC (2002) Methods to estimate the rock strength and tooth wear while drilling with roller-bits. *J Energy Resour Technol* 124:125–132
- Kovalyshen Y (2013) Self-excited axial vibrations of a drilling assembly: modeling and experimental investigation. In: the 47th US Rock Mechanics / Geomechanics Symposium, San Francisco, CA, USA 23–26
- Monjezi M, Amini Khoshalan H, Razifard M (2012) A Neuro-genetic network for predicting uniaxial compressive strength of rocks. *Geotech Geol Eng* 30:1053–1062
- Mostofi M, Rasouli V, Mawuli E (2011) An estimation of rock strength using a drilling performance model: a case study in Blacktip field, Australia. *Rock Mech Rock Eng* 44:305–316
- Panek LA, Fannon TA (1992) Size and shape effects in point load tests of irregular rock fragments. *Rock Mech Min Sci* 25:109–140
- Pincus H (1993) Round one—longitudinal and transverse pulse velocities, unconfined compressive strength, uniaxial elastic modulus, and splitting tensile strength. *Geotech Test J* 16(1):138–163
- Quane SL, Russell JK (2003) Rock strength as a metric of welding intensity in pyroclastic deposits. *Eur J Mineral* 15:855–864
- Singh VK, Singh DP (1993) Correlation between point load index and compressive strength for quartzite rocks. *Geotech Geol Eng* 11:269–272
- Singh TN, Kainthola A, Venkatesh A (2012) Correlation between point load index and uniaxial compressive strength for different rock types. *Rock Mech Rock Eng* 45:259–264
- Suzuki Y, Sasao H, Nishi K, Takesue K (1995) Ground exploration system using seismic cone and rotary percussion drill. *J Arch Build Sci* 1:180–184
- Tan ZY, Cai MF, Yue ZQ, Tham LG, Lee CF (2005) Application and reliability analysis of DPM system in site investigation of HK weathered granite. *J Univ Sci Technol Beijing* 12:481–488
- Tan ZY, Yue ZQ, Cai MF (2007) Analysis of energy for rotary drilling in weathered granite formation. *Chin J Rock Mech Eng* 26:478–483 (in Chinese)
- Teale R (1965) The concept of specific energy in rock drilling. *Int J Rock Mech Min Sci Geomech Abstr* 2:57–73
- Wijk G (1980) The uniaxial strength of rock material. *Geotech Test J* 3: 115–119
- Wyk GV, Els DNJ, Akdogan G, Bradshaw SM, Sacks N (2014) Discrete element simulation of tribological interactions in rock cutting. *Int J Rock Mech Min Sci* 65:8–19
- Yahiaoui M, Paris JY, Delbé K, Denape J, Gerbaud L, Dourfaye A (2016) Independent analyses of cutting and friction forces applied on a single polycrystalline diamond compact cutter. *Int J Rock Mech Min Sci* 85:20–26
- Yang WW, Yue ZQ, Tham LG (2012) Automatic monitoring of inserting or retrieving SPT sampler in drillhole. *Geotech Test J* 35:420–436
- Yaşar E, Ranjith PG, Viete DR (2011) An experimental investigation into the drilling and physico-mechanical properties of a rock-like brittle material. *J Pet Sci Eng* 76:185–193
- Yue ZQ, Lee CF, Law KT, Tham LG (2004) Automatic monitoring of rotary-percussive drilling for ground characterization—illustrated by a case example in Hong Kong. *Int J Rock Mech Min Sci* 41: 573–612